Published in final edited form as:
Sci Signal. ; 5(248): ra78. doi:10.1126/scisignal.2002936.

Mice Lacking the ITIM-Containing Receptor G6b-B Exhibit Macrothrombocytopenia and Aberrant Platelet Function

Alexandra Mazharian[#1], **Ying-Jie Wang**[#1,†], **Jun Mori**[1], **Danai Bem**[1], **Brenda Finney**[1], **Silke Heising**[1], **Paul Gissen**[2,‡], **James G. White**[3], **Michael C. Berndt**[4], **Elizabeth E. Gardiner**[5], **Bernhard Nieswandt**[6], **Michael R. Douglas**[7,8], **Robert D. Campbell**[9], **Steve P. Watson**[1], and **Yotis A. Senis**[1,§]

[1]Centre of Cardiovascular Sciences, Institute of Biomedical Research, School of Clinical and Experimental Medicine, College of Medical and Dental Sciences, University of Birmingham, Birmingham B15 2TT, UK [2]Department of Medical and Molecular Genetics, School of Clinical and Experimental Medicine, University of Birmingham, Birmingham B15 2TT, UK [3]Department of Laboratory Medicine and Pathology, University of Minnesota, Minneapolis, MN 55455, USA [4]Biomedical Diagnostics Institute, Dublin City University and Royal College of Surgeons in Ireland, Glasnevin, Dublin 9, Ireland [5]Australian Centre for Blood Diseases, Monash University, Alfred Medical Research and Education Precinct, Melbourne, Victoria 3004, Australia [6]University Hospital and Rudolf Virchow Center, DFG Research Center for Experimental Biomedicine, University of Würzburg, Würzburg 97080, Germany [7]Neuropharmacology and Neurobiology Section, School of Clinical and Experimental Medicine, University of Birmingham, Birmingham B15 2TT, UK [8]Department of Neurology, Dudley Group of Hospitals NHS Foundation Trust, Dudley DY1 2HQ, UK [9]Department of Physiology, Anatomy and Genetics, University of Oxford, Oxford OX1 3QX, UK

[#] These authors contributed equally to this work.

Abstract

Platelets are highly reactive cell fragments that adhere to exposed extracellular matrix (ECM) and prevent excessive blood loss by forming clots. Paradoxically, megakaryocytes, which produce platelets in the bone marrow, remain relatively refractory to the ECM-rich environment of the bone marrow despite having the same repertoire of receptors as platelets. These include the ITAM

[§]To whom correspondence should be addressed. y.senis@bham.ac.uk.
[†]Present address: Weatherall Institute of Molecular Medicine, University of Oxford, John Radcliffe Hospital, Headington, Oxford OX3 9DS, UK.
[‡]Present address: Medical Research Council Laboratory for Molecular Cell Biology, University College London, London WC1E 6BT, UK.

Author contributions: A.M. and Y.-J.W. designed and performed the experiments; collected, analyzed, and interpreted the data; and participated in writing and revising the paper. J.M. designed and performed the experiments; collected, analyzed, and interpreted the data; and participated in revising the paper. D.B. designed and performed the experiments; collected, analyzed, and interpreted the data; and participated in writing the paper. B.F. designed the experiments and interpreted the data. S.H. collected, analyzed, and interpreted the data. P.G. participated in revising the manuscript. J.G.W. analyzed and interpreted the data. M.C.B. provided a custom antibody. E.E.G. provided a custom antibody and revised the manuscript. B.N. provided a custom antibody. M.R.D. generated a custom antibody and revised the manuscript. R.D.C. contributed intellectually and revised the manuscript. S.P.W. contributed intellectually and revised the manuscript. Y.A.S. was responsible for the overall supervision of the study; designed and performed the experiments; collected, analyzed, and interpreted the data; and wrote and revised the paper.

Competing interests: The authors declare that they have no competing interests.

Europe PMC Funders Author Manuscripts

(immunoreceptor tyrosine–based activation motif)–containing collagen receptor complex, which consists of glycoprotein VI (GPVI) and the Fc receptor γ-chain, and the ITIM (immunoreceptor tyrosine–based inhibition motif)–containing receptor G6b-B. We showed that mice lacking G6b-B exhibited macrothrombocytopenia (reduced platelet numbers and the presence of enlarged platelets) and a susceptibility to bleeding as a result of aberrant platelet production and function. Platelet numbers were markedly reduced in G6b-B–deficient mice compared to those in wild-type mice because of increased platelet turnover. Furthermore, megakaryocytes in G6b-B–deficient mice showed enhanced metalloproteinase production, which led to increased shedding of cell-surface receptors, including GPVI and GPIba. In addition, G6b-B–deficient megakaryocytes exhibited reduced integrin-mediated functions and defective formation of proplatelets, the long filamentous projections from which platelets bud off. Together, these findings establish G6b-B as a major inhibitory receptor regulating megakaryocyte activation, function, and platelet production.

INTRODUCTION

Platelets are small anucleate blood cell fragments that play a vital role in hemostasis (the cessation of bleeding) and thrombosis (formation of blood clots in blood vessels) (1, 2), which they perform by adhering to exposed extracellular matrix (ECM) at sites of vascular injury and forming a hemostatic plug that prevents excessive blood loss. Platelets have a life span of 7 to 10 days in humans and 3 to 5 days in mice (3, 4). New platelets are constantly produced to maintain a normal range of biologically active platelets in the circulation (150×10^3 to 400×10^3 platelets/μl in humans and 700×10^3 to 1500×10^3 platelets/μl in mice) (1). Old, defective, and preactivated platelets are rapidly cleared from the circulation by resident macrophages in the spleen and liver (3).

A key yet unresolved question is how megakaryocytes, bone marrow cells that produce platelets, remain relatively refractory in the ECM-rich environment of the bone marrow despite having the same repertoire of cell-surface receptors as platelets. One potential pathway responsible for this difference is through immunoreceptor tyrosine–based inhibition motif (ITIM)–containing receptors, which inhibit activation signals (5). ITIMs, which have the consensus sequence (I/V/L/S)xYxx(L/V), are phosphorylated by Src family kinases (SFKs) and act as docking sites for SHIP-1 [Src homology 2 (SH2) domain–containing inositol-5-phosphatase-1] and the structurally related nontransmembrane protein-tyrosine phosphatases Shp1 and Shp2 (SH2 domain–containing protein-tyrosine phosphatases 1 and 2), which dephosphorylate key components of activation pathways (5). Platelets have several ITIM-containing receptors, including platelet-endothelial cell adhesion molecule-1 (PECAM-1) (6), carcinoembryonic antigen–related cell adhesion molecule 1 (CEACAM1) (7), triggering receptor expressed on myeloid cell–like transcript-1 (TLT-1) (8), and G6b-B (9). The ITIM-containing collagen receptor LAIR-1 [leukocyte-associated immunoglobulin (Ig)–like receptor-1] is found in hematopoietic stem cells and immature megakaryocytes but not in platelets (10, 11). Unique among this group of ITIM-containing receptors is G6b-B, which is highly abundant in megakaryocytes and platelets (12, 13) and is constitutively phosphorylated and associated with Shp1 and Shp2 (9, 14, 15). G6b-B inhibits signaling from the immunoreceptor tyrosine–based activation motif (ITAM)–containing collagen activation receptor complex GPVI–FcR γ-chain (glycoprotein VI–Fc receptor γ-chain) and

the hemITAM-containing podoplanin activation receptor CLEC-2 (C-type lectin-like receptor 2) in transiently transfected DT40 chicken B cells (16), as well as GPVI- and adenosine diphosphate (ADP)–induced platelet aggregation after antibody-mediated cross-linking (17).

We investigated the physiological function of G6b-B through the use of a *G6b* knockout mouse model. Unexpectedly, G6b-B–deficient mice were markedly macrothrombocytopenic and had a bleeding diathesis because of defective platelet production and function. Ablation of GPVI and CLEC-2 partially rescued the phenotype of G6b-B–deficient mice, suggesting that tonic signaling through these receptors contributed to the defect. Thus, we suggest that G6b-B is a previously uncharacterized regulator of megakaryocyte activation and function and platelet production.

RESULTS

Mouse and human G6b-B are differentially glycosylated

We characterized G6b-B in mouse megakaryocytes and platelets to serve as a basis for the generation of a G6b-B–deficient mouse model. Mouse *G6b*, the gene that encodes G6b-B, is located in the major histocompatibility complex region of chromosome 17 (18) and is predicted to encode a 242–amino acid protein with the same structural features as human G6b-B, including a single extracellular variable Ig domain, a single transmembrane domain, and a cytoplasmic tail containing an ITIM and an ITSM [immunoreceptor tyrosine–based switch motif; consensus sequence: TxYxx(V/I)] in its C terminus (figs. S1 and S2). G6b-B is highly abundant in mature mouse bone marrow–derived megakaryocytes and platelets but not in immature megakaryocytes (fig. S3, A and B). However, unlike human G6b-B, which migrates as two distinct bands at 24 to 30 kD when analyzed by SDS–polyacrylamide gel electrophoresis (fig. S3B, right), mouse G6b-B migrates as a smear in the range of 40 to 45 kD (fig. S3B, left), which is a result of differential glycosylation because deglycosylation with peptide *N*-glycosidase F (PNGase F) caused human and mouse G6b-B to migrate with their predicted molecular masses of ~24 kD (fig. S3B). Human and mouse G6b-B were constitutively tyrosine-phosphorylated and associated with Shp1 and Shp2 in mouse megakaryocytes (fig. S3C, right) and in mouse and human platelets [fig. S3, C (left) and D] (9, 17). Tyrosine phosphorylation of G6b-B and its interactions with Shp1 and Shp2 were marginally enhanced in collagen-stimulated platelets, and both sets of responses were inhibited in the presence of the SFK inhibitor PP1 (4-amino-5-(4-methylphenyl)-7-(*t*-butyl)pyrazolo[3,4-*d*]-pyrimidine) [fig. S3, C (left) and D].

G6b$^{-/-}$ mice exhibit severe macrothrombocytopenia and have abnormal platelets

We generated *G6b*-deficient mice by crossing *G6b*$^{flox/flox}$ mice, in which the entire *G6b* gene (exons 1 to 6) was flanked by *loxP* sites (fig. S4), with *Gt(ROSA)26Sor*$^{tm16(Cre)Arte}$ mice, resulting in ablation of *G6b* in all tissues (fig. S4). Homozygous *G6b* knockout mice (*G6b*$^{-/-}$) were born at Mendelian frequencies, were fertile, and survived for >25 weeks with no overt growth or developmental defects. G6b-B was not detectable in mature megakaryocytes or platelets from *G6b*$^{-/-}$ mice by flow cytometry or Western blotting analysis (Fig. 1A). Hematological analysis revealed that *G6b*$^{-/-}$ mice were markedly

macrothrombocytopenic (Fig. 1B and table S1). The mean platelet count of *G6b*$^{-/-}$ mice was reduced by 77% and the mean platelet volume was increased by 38% compared with age-matched wild-type control mice (*G6b*$^{+/+}$) (Fig. 1B and table S1). Increased platelet volume is indicative of immature platelets (19, 20).

G6b$^{-/-}$ mice show increased platelet turnover and extramedullary hematopoiesis

The marked reduction in platelet counts in *G6b*$^{-/-}$ mice suggested a major defect in platelet clearance, production, or both. Thus, we measured platelet half-life in *G6b*$^{-/-}$ mice, as previously described (21). Briefly, mice were given a single intravenous injection of biotin-*N*-hydroxysuccinimide, which biotinylates primary amines in glycoproteins on the platelet surface, and then we quantified by flow cytometry the percentages of biotinylated platelets (biotin$^{+}\alpha_{IIb}\beta_3{}^{+}$) remaining in the blood at various days after injection. We found that platelet half-life was reduced to 33 hours in *G6b*$^{-/-}$ mice, compared with 64 hours in age-matched wild-type mice, demonstrating a substantial increase in platelet clearance in the *G6b*$^{-/-}$ mice (Fig. 2A). A large proportion of platelets in *G6b*$^{-/-}$ mice were IgG- and IgM-positive (Fig. 2B), which suggested the existence of an anti-platelet antibody–mediated response and the enhanced clearance of opsonized platelets through the mononuclear phagocyte system (3).

The rate of platelet recovery after platelet depletion that was triggered by an anti-GPIbα antibody was reduced in *G6b*$^{-/-}$ mice compared to that in wild-type mice (Fig. 2C), suggesting reduced platelet production. However, this is complicated by the increased platelet clearance observed in these mice (Fig. 2A). The spleen, which acts as a site of platelet clearance and production in cases of bone marrow damage, such as myelofibrosis (22), was moderately enlarged in *G6b*$^{-/-}$ mice compared to that in control mice (fig. S5A). Clusters of megakaryocytes in the bone marrow and red pulp of *G6b*$^{-/-}$ mice suggested that myelofibrosis and extramedullary hematopoiesis had occurred (fig. S5B). Indeed, the reticulin stain revealed increased fibrosis in the bone marrow and spleen of mutant mice compared to control mice (fig. S5B, bottom). Increased numbers of megakaryocytes in *G6b*$^{-/-}$ mice were likely a result of an increase in the concentration of thrombopoietin (Tpo) in the plasma (fig. S5C), which is inversely related to platelet counts (23). Together, these findings suggest a futile cycle of rapid antibody-mediated platelet clearance and aberrant platelet production in *G6b*$^{-/-}$ mice, resulting in a net deficit in circulating platelet counts.

G6b$^{-/-}$ mice exhibit abnormal megakaryocyte function and proplatelet formation

We next searched for further evidence of reduced platelet production in *G6b*$^{-/-}$ mice. We analyzed bone marrow–derived megakaryocytes from *G6b*$^{-/-}$ mice for developmental and functional defects. G6b-B–deficient megakaryocytes survived and grew normally in vitro, with normal ploidy (fig. S6A) and $\alpha_{IIb}\beta_3$ surface abundance (fig. S6B and Table 1), suggesting no overt developmental defects. However, the abundances of GPVI, the α_2 integrin subunit, and GPIbα in mature G6b-B–deficient megakaryocytes were substantially reduced compared to those in wild-type megakaryocytes (fig. S6B and Table 1). In contrast, the abundance of the metalloproteinase ADAM-10, which causes shedding of GPVI and the GPIbα subunit, which provides the von Willebrand factor binding site in the GPIb-IX-V receptor complex (24, 25), was increased in mature G6b-B–deficient megakaryocytes compared to that in wild-type cells (fig. S6B and Table 1).

Despite having normal amounts of $\alpha_{IIb}\beta_3$, G6b-B–deficient megakaryocytes exhibited a marked reduction in spreading on fibrinogen- or fibronectin-coated surfaces (Fig. 3, A and B, left), suggesting defective outside-in integrin signaling. Reduced spreading on collagen was likely partially a result of the reduced amounts of GPVI and α_2 integrin (Fig. 3, A and B, left, and Table 1). Wild-type megakaryocytes maintained under the same conditions for longer periods (5 hours) formed long filamentous proplatelet projections from which platelets bud off (Fig. 3, A and B, right) (19). G6b-B–deficient megakaryocytes formed fewer and less highly branched proplatelets on fibrinogen- or fibronectin-coated surfaces than did control megakaryocytes (Fig. 3, A and B, right), suggesting defective microtubule extension and actin-mediated branching (26). Neither wild-type nor G6b-B–deficient megakaryocytes formed proplatelets on collagen-coated surfaces (Fig. 3, A and B, right), as was anticipated, because collagen is reported to inhibit proplatelet formation in vitro (27).

Western blotting analysis with phospho-specific antibodies revealed substantial reductions in the extent of phosphorylation of the activation loop tyrosine of SFKs [Src phosphorylated at Tyr^{418} ($pTyr^{418}$)] and extracellular signal–regulated kinases 1 and 2 (ERK1/2; $pThr^{202}$ and $pTyr^{204}$ in ERK1 and $pThr^{185}$ and $pTyr^{187}$ in ERK2) downstream of $\alpha_{IIb}\beta_3$ in fibrinogen-adherent, G6b-B–deficient megakaryocytes compared to wild-type megakaryocytes (Fig. 3C, left). Phosphorylation of these sites is required for maximal activation of these kinases (28, 29). Src is required for the initiation and propagation of outside-in $\alpha_{IIb}\beta_3$ signaling, whereas ERK1/2 activation is a distal signaling event in the Ras–mitogen-activated protein kinase pathway that has been implicated in cell survival, growth, and development (30). SFK phosphorylation was also reduced in Tpo-stimulated G6b-B–deficient megakaryocytes; however, Tpo-mediated ERK1/2 phosphorylation was normal, consistent with the normal growth and ploidy of these cells (Fig. 3C, right). Tpo is the main cytokine that stimulates megakaryocytes to produce platelets. These findings demonstrate the specificity of G6b–B in regulating outside-in integrin $\alpha_{IIb}\beta_3$ signaling relative to Tpo receptor (Mpl) signaling. Altered outside-in integrin signaling likely contributes to the functional defects exhibited by G6b-B–deficient megakaryocytes in vitro and in vivo, as previously reported (30-33).

G6b$^{-/-}$ mice exhibit increased bleeding and aberrant platelet function

Platelets from *G6b*$^{-/-}$ mice tended to be larger and more ovoid-shaped compared with platelets from *G6b*$^{+/+}$ mice (fig. S7), consistent with increased platelet turnover and the presence of immature platelets. In addition, platelets from *G6b*$^{-/-}$ mice also had altered organelle and granule content (fig. S7), consistent with aberrant platelet production (34). Surface glycoprotein abundance was also defective in G6b-B–deficient platelets (Fig. 4), which correlated with altered glycoprotein amounts in G6b-B–deficient megakaryocytes (fig. S6B). The amounts of GPVI on mutant platelets were reduced by 82% compared to those in wild-type platelets (Fig. 4), whereas the amounts of α_2 integrin, GPIbα, and CLEC-2 were reduced by 18, 13, and 6%, respectively (Fig. 4). In contrast, ADAM-10 abundance was 36% greater in G6b-B–deficient platelets than in wild-type platelets (Fig. 4).

Not surprisingly, *G6b*$^{-/-}$ mice bled excessively after receiving a tail injury (fig. S8A). Platelets from *G6b*$^{-/-}$ mice adhered poorly and failed to form normal aggregates on collagen-coated surfaces under arterial shear rates (1000 s^{-1}) (fig. S8B). Aggregates were

unstable and tended to fragment with time. We also performed platelet function tests in vitro with equal numbers of washed platelets. We measured GPVI-mediated aggregation and adenosine triphosphate (ATP) secretion from dense granules in response to the GPVI-specific synthetic peptide collagen-related peptide (CRP), the snake toxin convulxin, which binds to GPVI and GPIbα, and the physiological ligand collagen, which binds to GPVI and the integrin $\alpha_2\beta_1$. Platelets from *G6b*$^{-/-}$ mice did not aggregate or secrete ATP in response to high concentrations (30 μg/ml) of either CRP or convulxin, consistent with the reduction in GPVI abundance on their surface (Fig. 5A, Table 2, and fig. S9). The amount of cell-surface P-selectin, a marker of α-granule secretion, and the extent of fibrinogen binding, a marker of inside-out signaling and integrin function, were also reduced in CRP-stimulated G6b-B–deficient platelets compared to those in stimulated wild-type platelets (Fig. 5B). In contrast, G6b-B–deficient platelets responded weakly to an intermediate concentration of collagen (3 μg/ml), which signals through GPVI and the $\alpha_2\beta_1$ integrin (Fig. 5A, Table 2, and fig. S9) (35, 36). This suggests that there was a sufficient amount of $\alpha_2\beta_1$ to cause activation of GPVI through a vidity despite the reduction in GPVI abundance, as previously reported (37). In contrast, platelets from *G6b*$^{-/-}$ mice exhibited enhanced reactivity to an anti–CLEC-2 antibody (Fig. 5A), which signals through a hemITAM sequence and the SFK–Syk–phospholipase C γ2 (PLC-γ2) signaling pathway (38). Thus, the defect in the response to GPVI agonists can be explained by the marked reduction in the abundance of the glycoprotein receptor, whereas enhanced CLEC-2 responses were likely mediated by increased signaling in the absence of inhibition by G6b-B.

Platelets from *G6b*$^{-/-}$ mice responded normally to the thromboxane A_2 (TxA_2) analog U46619 (10 μM), which signals through the G_q-coupled TxA_2 receptor (Fig. 5A), and an intermediate concentration of ADP (10 μM), which signals through the G_q-coupled $P2Y_1$ and G_i-coupled $P2Y_{12}$ receptors (Fig. 5A). However, G6b-B–deficient platelets exhibited reversible aggregation and reduced ATP secretion in response to an intermediate concentration (0.06 U/ml) of thrombin, which signals through the G_q-coupled protease-activated receptor-4 (PAR-4) (Fig. 5A). Consistent with these findings, the cell-surface abundance of P-selectin was also reduced in response to thrombin (for both 0.06 and 0.6 U/ml), whereas fibrinogen binding was only reduced in response to a lower concentration of thrombin (Fig. 5B).

We also analyzed the ability of G6b-B–deficient platelets to adhere to and spread on a fibrinogen-coated surface (Fig. 5, C and D), which is an $\alpha_{IIb}\beta_3$-mediated event that is dependent on outside-in signaling through the SFK–Syk–PLC-γ2 signaling pathway (39). We previously reported an increase in the extent of G6b-B phosphorylation in fibrinogen-spread human platelets (15), which suggested that G6b-B might regulate outside-in integrin signaling. We found that G6b-B–deficient platelets spread normally on fibrinogen under basal conditions but showed a marked reduction in lamellipodia formation when the platelets were preactivated with thrombin (0.1 U/ml; Fig. 5, C and D), consistent with the reduced thrombin reactivity described earlier (Fig. 5, A and B). Under these conditions, less than half of G6b-B–deficient platelets formed lamellipodia (Fig. 5, C and D).

Syk is constitutively activated in *G6b*$^{-/-}$ platelets

We next checked for biochemical evidence of platelet preactivation. Our previous findings showed that G6b-B inhibits constitutive signaling from GPVI and CLEC-2 in transiently transfected DT40 chicken B cells (16). We analyzed the phosphorylation status of the tyrosine kinase Syk and the ITAM-containing FcR γ-chain in resting G6b-B–deficient platelets by immunoprecipitation and Western blotting analysis. We found that the phosphorylation of Syk was enhanced in resting G6b-B–deficient platelets compared to that in wild-type platelets, suggesting that Syk activity was increased (Fig. 6A, top). This finding was confirmed with a phospho-specific antibody that recognized activated Syk (pTyr$^{519/520}$) (Fig. 6B). However, the FcR γ-chain was phosphorylated to the same extent in control and G6b-B–deficient platelets, making it unlikely that this was the cause of the increase in Syk activity (Fig. 6C). Moreover, less phosphorylated FcR γ-chain co-immunoprecipitated with Syk from resting G6b-B–deficient platelets than with Syk from wild-type platelets (Fig. 6A, bottom). Despite the extent of Syk phosphorylation being increased in G6b-B–deficient platelets compared to that in wild-type platelets, SFK and PLC-γ2 were phosphorylated to the same extent in control and mutant platelets under these conditions (fig. S10A).

The extent of tyrosine phosphorylation of several bands was enhanced in resting G6b-B–deficient platelets compared to that in wild-type platelets, including bands corresponding to proteins of 25 and 116 kD (figs. S10B and S11). Phosphorylation of SFKs was normal in resting and collagen-stimulated G6b-B–deficient platelets in the presence of indomethacin, apyrase, and lotrafiban, which inhibit cyclooxygenase, ADP, and $\alpha_{IIb}\beta_3$, respectively (fig. S11), despite G6b-B–deficient platelets having reduced cell-surface abundance of GPVI and α_2 integrin (Table 2). This finding suggested that SFK activity in G6b-B–deficient platelets was normal. Phosphorylation of Syk was also normal in resting G6b-B–deficient platelets under these conditions (fig. S11), suggesting that the inhibitors prevented Syk from becoming preactivated. However, tyrosine phosphorylation of the FcR γ-chain, Syk, and PLC-γ2, downstream of SFKs, was markedly reduced in collagen-stimulated G6b-B–deficient platelets compared to that in stimulated control platelets (fig. S11). The extent of tyrosine phosphorylation remained unchanged in CRP-stimulated G6b-B–deficient platelets, including an apparently hyperphosphorylated band migrating at 25 kD (fig. S10). These findings demonstrate the enhanced phosphorylation at a critical point downstream of platelet surface glycoprotein receptors, namely, the tyrosine kinase Syk, which may contribute to platelet preactivation and potentiation of the response to CLEC-2.

G6b$^{-/-}$ mice show increased GPVI and GPIbα shedding

We next investigated the cause of the reduced GPVI and GPIbα abundance in G6b-B–deficient platelets. Potential causes included reduced transcription of the genes encoding these receptors, as well as increased internalization and shedding of the receptor proteins. Another possibility was a reduction in the abundance of the FcR γ-chain, which is required for the cell-surface expression of GPVI (40). To test these possibilities, we analyzed whole-cell lysates of resting platelets by Western blotting for GPVI and the FcR γ-chain. The anti-GPVI antibody that we used was directed against the cytoplasmic tail of GPVI, so it could detect both full-length GPVI (62 kD) and the sheddase-generated C-terminal tail (8 kD). The amount of intact GPVI was markedly reduced in G6b-B–deficient platelets compared to that

in wild-type platelets (Fig. 7A, left), whereas the sheddase-generated C-terminal tail was increased in abundance (Fig. 7A, left), consistent with enhanced GPVI shedding. FcR γ-chain abundance was also reduced in G6b-B–deficient platelets compared to that in wild-type platelets (Fig. 7A, middle), contributing to an overall reduction in the amount of GPVI at the cell surface. Because GPIbα is cleaved by the same sheddases that cleave GPVI, namely, ADAM-10 and ADAM-17 (24, 25), we checked for evidence of enhanced GPIbα shedding in *G6b*$^{-/-}$ mice. Indeed, we found that the sheddase-generated extracellular region of GPIbα, which is referred to as glycocalicin, was increased in abundance in the plasma of *G6b*$^{-/-}$ mice compared to that in wild-type mice (Fig. 7A, right).

Consistent with the model of enhanced shedding of GPVI and GPIbα in *G6b*$^{-/-}$ mice, the cell-surface amounts of GPVI and GPIbα were both reduced by 64% in $\alpha_{IIb}\beta_3{}^+$ G6b-B–deficient bone marrow cells (fig. S12), and ADAM-10 abundance was increased by 35% (fig. S12). Concomitantly, we observed a 55% increase in the proportion of P-selectin$^+\alpha_{IIb}\beta_3{}^+$ cells in the bone marrow of *G6b*$^{-/-}$ mice compared to that in wild-type mice, which was suggestive of increased megakaryocyte preactivation (fig. S12), consistent with enhanced shedding and myelofibrosis (Fig. 7A and fig. S5B).

Ablation of GPVI and CLEC-2 partially rescues macrothrombocytopenia in *G6b*$^{-/-}$ mice

To test the hypothesis that tonic GPVI and CLEC-2 signaling was the underlying cause of macrothrombocytopenia in *G6b*$^{-/-}$ mice, we generated *G6b* and *Gp6* double-knockout (DKO) mice and ablated CLEC-2 through antibody-induced down-regulation (41). Platelet counts and volumes were normal in *Gp6*$^{-/-}$ mice (Fig. 7B and table S2), as expected (42). Platelets counts were 54% higher in *G6b/Gp6* DKO mice (Fig. 7B and table S2) than in *G6b*$^{-/-}$ mice (Fig. 1B and table S1), and cell-surface glycoprotein abundance was normal in *G6b/Gp6* DKO platelets, except for the α_2 integrin subunit, which was reduced (fig. S13), demonstrating a partial rescue of the platelet phenotype in *G6b/Gp6* DKO. A further 87% increase in platelet counts was observed in *G6b/Gp6* DKO mice treated with anti–CLEC-2 antibody compared with that in *G6b/Gp6* DKO mice treated with IgG isotype control antibody (Fig. 7C). Platelet counts were made 10 days after antibody injection, when platelet counts had stabilized after their initial antibody-mediated depletion (figs. S14 and S15), and the amount of CLEC-2 was still substantially reduced compared to that of control mice (figs. S14 and S15). These findings demonstrate a further rescue of platelet counts after loss of CLEC-2.

To circumvent the reduction in GPVI abundance in G6b-B–deficient platelets and to demonstrate the inhibitory effect of G6b-B on GPVI function, we analyzed platelets from *G6b*$^{+/-}$*Gp6*$^{+/-}$ mice. *G6b*$^{+/-}$*Gp6*$^{+/-}$ mice had normal platelet counts and volumes (fig. S16A); however, platelets from *G6b*$^{+/-}$*Gp6*$^{+/-}$ mice, which had 50% of the normal amounts of G6b-B and GPVI (fig. S16B), exhibited enhanced reactivity to collagen and CRP compared with platelets from *Gp6*$^{+/-}$ mice (fig. S17), which had 50% GPVI abundance (fig. S16B). Platelets from *G6b*$^{+/-}$*Gp6*$^{+/-}$ mice responded normally to thrombin (fig. S17). These findings provide evidence that G6b-B is an inhibitor of GPVI-mediated functional responses in platelets.

DISCUSSION

Our findings suggest that G6b-B acts as a critical regulator of megakaryocyte function and platelet production. G6b-B–deficient mice are markedly macrothrombocytopenic and exhibited a bleeding diathesis because of aberrant platelet production and function. Platelet counts were substantially reduced in G6b-B–deficient mice compared to those in wild-type mice as a result of increased platelet turnover. In addition, megakaryocytes from G6b-B–deficient mice exhibited reductions in integrin-mediated functions and proplatelet formation. Several lines of evidence point to G6b-B being an inhibitor of megakaryocytes in the bone marrow, including the enhanced GPVI and GPIbα shedding and enhanced platelet reactivity to anti–CLEC-2 antibody in *G6b*$^{-/-}$ mice. In addition, platelets from *G6b*$^{+/-}$*Gp6*$^{+/-}$ mice responded better to CRP and collagen than did platelets from *Gp6*$^{+/-}$ mice. However, tonic GPVI and CLEC-2 signaling does not fully explain the macrothrombocytopenia in *G6b*$^{-/-}$ mice. A similar phenotype is not observed in mice lacking other megakaryocyte or platelet ITIM-containing receptors, namely, PECAM-1 (6, 43, 44), CEACAM1 (7), TLT-1 (8), and LAIR-1 (45), demonstrating the distinct functional role of G6b-B in megakaryocytes and platelets.

The cause of the severe macrothrombocytopenia in *G6b*$^{-/-}$ mice was a combination of enhanced platelet clearance and reduced platelet production. Enhanced platelet clearance was a result of antibody-dependent and antibody-independent mechanisms, similar to that seen in Wiskott-Aldrich syndrome protein (WASp) and WASp-interacting protein (WIP) deficiencies in humans and mice (46, 47). WIP-deficient mice are concomitantly WASp-deficient and develop platelet-associated IgA, which normalizes platelet survival and diminishes GPVI-mediated responses (47). Here, we demonstrated that G6b-B–deficient mice also developed platelet-associated Igs, which likely target defective platelets for destruction by the mononuclear phagocyte system. We suspect that platelet-associated antibodies recognize aberrantly folded or glycosylated glycoproteins on the platelet surface. The presence of both IgM and IgG on the surface of G6b-B–deficient platelets suggests the existence of acute and prolonged immune responses, respectively.

We identified several antibody-independent causes of macrothrombocytopenia in *G6b*$^{-/-}$ mice, including reduced GPIbα abundance, integrin-mediated functional responses, and proplatelet formation. We do not believe that reduced GPIbα abundance is the underlying cause of the defect because GPIbα amounts were only marginally reduced in G6b-B–deficient megakaryocytes as a result of enhanced shedding. More likely explanations are aberrant integrin-mediated functional responses, signaling defects, and reduced proplatelet formation, all of which have been associated with abnormal platelet counts (30, 32, 33, 48, 49). According to the current model of platelet production, megakaryocyte progenitors must migrate from the osteoblastic niche to the vascular niche, where they extend proplatelets into the vascular lumen, and then release platelets into the circulation (50). The migration process is dependent on the integrin $\alpha_{IIb}\beta_3$ and its associated signaling pathway (33, 48). G6b-B–deficient megakaryocytes exhibited substantial reductions in integrin-mediated spreading and proplatelet formation in vitro. We suspect that the reduction in proplatelet formation was a result of aberrant signaling regulating microtubule extension and actin-mediated branching, possibly at the level of small guanosine triphosphatases and actin-

associated mediators of cytoskeletal remodeling (51). The defect in proplatelet formation does not seem to be a result of a developmental defect because ploidy, $\alpha_{IIb}\beta_3$ abundance, and Tpo-mediated ERK1/2 activation were normal in G6b-B–deficient megakaryocytes, despite having a reduction in SFK activation.

Ablation of the activation receptors GPVI and CLEC-2 partially rescued the thrombocytopenia in G6b-B–deficient mice, which suggests that tonic signaling through these receptors contributes to this phenotype. This is consistent with our model in which G6b-B is an inhibitor of GPVI and CLEC-2 signaling and maintains megakaryocytes and platelets in an inactive state. Thus, megakaryocytes and platelets would be more prone to preactivation in the absence of G6b-B, resulting in megakaryocytes remaining in the osteoblastic niche and releasing fewer platelets into the circulation. This idea was supported by our observation of increased numbers of P-selectin–positive megakaryocytes in the bone marrow of G6b-B–deficient mice compared to those of wild-type mice, leading to megakaryocyte-mediated bone marrow destruction and myelofibrosis. Increased ADAM-10 amounts may act as a mechanism to suppress activation signals in megakaryocytes and platelets. GPVI shedding normally takes place after platelet activation and is mediated by the metalloproteinases ADAM-10 and ADAM-17 (24, 25). ADAM-17 also mediates the constitutive and regulated shedding of GPIbα (52). We suspect that preactivated and defective platelets are being rapidly cleared from the circulation.

The bleeding diathesis exhibited by *G6b*$^{-/-}$ mice was a result not only of reduced platelet counts but also of reduced platelet reactivity to collagen and thrombin. The reduced reactivity to collagen was primarily due to down-regulation of the GPVI-FcR γ-chain and $\alpha_2\beta_1$ integrin; however, the cause of the reduced thrombin reactivity remains undefined. We speculate that this may have been due to down-regulation of the thrombin receptor PAR-4, reduced receptor signaling, or reduced secretion of the secondary mediators ADP and TxA_2. Further investigation is required to elucidate the exact cause of this defect.

The enhanced phosphorylation of Syk in resting G6b-B–deficient platelets suggested that they were primed for activation. Despite the enhanced phosphorylation of Syk under resting conditions, the extent of phosphorylation was reduced in collagen-stimulated platelets, consistent with reduced amounts of GPVI-FcR γ-chain and α_2 integrin. Not surprisingly, the extent of PLC-γ2 phosphorylation downstream of Syk was also reduced. Although we could not detect phosphorylated linker of activated T cells (LAT) in resting platelets, we found a band corresponding to the molecular mass of LAT that was reduced in phosphorylation in collagen-stimulated G6b-B–deficient platelets. However, SFKs, which lie upstream of Syk and regulate its activity and compartmentalization, were phosphorylated to the same extent in control and G6b-B–deficient platelets. On the basis of these findings, we hypothesize that G6b-B directly regulates Syk activity or a Syk-docking site at the plasma membrane. We believe that it does so by maintaining active Shp1 and Shp2 at the plasma membrane. It is well established that simultaneous occupancy of both SH2 domains of Shp2 with ligands containing tandem phosphotyrosine residues increases Shp2 activity (53-56). Structural and enzymological similarities between Shp1 and Shp2 suggest that Shp1 is regulated in an analogous manner (57, 58). The Syk-docking site that we hypothesize is dephosphorylated by G6b-B-associated Shp1 and Shp2 does not seem to be the ITAM-containing FcR γ-chain

but rather the hemITAM-containing CLEC-2 receptor. This would also explain the hyperreactivity of G6b-B–deficient platelets to antibody-mediated CLEC-2 activation.

In conclusion, we suggest that G6b-B is a major regulator of megakaryocyte function and platelet production, and that its absence results in a complex phenotype that includes macrothrombocytopenia and a platelet-based bleeding diathesis. Investigation of G6b-B should be extended to human patients with inherited thrombocytopenias and platelet-based bleeding disorders, a substantial proportion of which are unclassified.

MATERIALS AND METHODS

Mice

G6b$^{flox/flox}$ mice were generated on a C57BL/6 background by TaconicArtemis as outlined in fig. S4. *G6b* constitutive knockout mice were generated by crossing *G6b*$^{flox/flox}$ mice (in which exons 1 to 6 are flanked by *loxP* sites) with *Gt(ROSA)26Sor*$^{tm16(Cre)Arte}$ knock-in mice. GPVI-deficient (*Gp6*$^{-/-}$) mice on a C57BL/6 background were provided by J. Ware (University of Arkansas) (42). G6b-B/GPVI DKO mice were generated by crossing *G6b*$^{-/-}$ mice with *Gp6*$^{-/-}$ mice. All procedures were undertaken with the U.K. Home Office approval in accordance with the Animals (Scientific Procedures) Act of 1986.

Antibodies

Rabbit polyclonal antibody against mouse G6b-B was raised against the cytoplasmic tail of mouse G6b-B (Eurogentec). Rat anti-mouse G6b-B monoclonal antibody was raised against a mouse G6b-B extracellular domain Fc fusion protein (Biogenes). Rabbit anti-mouse GPVI polyclonal antibody was raised against the cytoplasmic tail of mouse GPVI. Carboxyfluorescein-conjugated monoclonal anti-mouse ADAM-10 antibody was from R&D Systems. Anti-pERK1/2 (Thr^{202}/Tyr^{204}) and anti-ERK1/2 antibodies were from Santa Cruz Biotechnology. All other antibodies were sourced as previously described (9, 30, 33, 48, 59).

Chemicals

All reagents were sourced as previously described (9, 30, 33, 48, 59).

Preparation and culture of mouse megakaryocytes

Mature megakaryocytes from mouse bone marrow were defined as the population of cells generated with the methodology previously described (33, 60, 61).

Measurement of platelet half-life

Platelet half-life was measured as previously described (21, 62). Whole blood was collected from mice at various times after they were subjected to intravenous injection with 150 μl of biotin-*N*-hydroxysuccinimide (4 mg/ml) in buffer containing 10% fetal bovine serum and 5 mM EDTA, which biotinylates primary amines in surface glycoproteins. Platelets were stained with fluorescein isothiocyanate (FITC)–conjugated anti-mouse $\alpha_{IIb}\beta_3$ antibody and streptavidin-phycoerythrin (PE) for 1 hour on ice, and the percentage of biotin-labeled $\alpha_{IIb}\beta_3^+$ platelets was measured by flow cytometry.

Immune thrombocytopenia

Thrombocytopenia was induced in 8- to 12-week-old *G6b*$^{+/+}$ and *G6b*$^{-/-}$ mice by intraperitoneal injection of anti-mouse GPIbα antibody (2 μg/g weight of mouse), as previously described (59).

Antibody-mediated CLEC-2 depletion

Eight- to 12-week-old *G6b*$^{+/+}$*Gp6*$^{+/+}$ and *G6b*$^{-/-}$*Gp6*$^{-/-}$ mice were given an intravenous injection of anti-mouse CLEC-2 antibody (INU-1, 8 μg/g weight of mouse) or the same dose of rat IgG1 isotype control antibody, as previously described (41). Blood samples were collected 0 to 10 days after injection. Platelet counts and volumes were measured with an ABX Pentra 60 Hematology Analyzer (Block Scientific Inc.), and surface CLEC-2 abundance was measured by flow cytometry.

Immunohistochemistry

Femora and spleens from *G6b*$^{+/+}$ and *G6b*$^{-/-}$ mice were fixed in buffered formalin and embedded in paraffin. Sections (5 μm) were stained by hematoxylin and eosin and then examined with a Zeiss Axiovert 200 inverted high-end microscope.

Analysis of megakaryocyte surface glycoprotein abundance and ploidy

Bone marrow cells flushed from the femora and tibia of mice were double-stained with FITC–anti-GPVI and PE–anti-α_{IIb} antibodies and quantified by flow cytometry. Surface amounts of α_{IIb}, GPIbα, GPVI, and α_2 integrin were measured on cultured bone marrow–derived megakaryocytes by flow cytometry with FITC-conjugated primary antibodies. The DNA ploidy of mature megakaryocytes isolated by BSA gradient was analyzed after anti-α_{IIb} staining and DNA staining with propidium iodide (10 μg/ml). Cells positive for α_{IIb} were gated to analyze DNA content.

Megakaryocyte spreading and proplatelet formation

Mature megakaryocytes were plated on fibrinogen-, fibronectin-, or collagen-coated surfaces at 37°C, and spreading and proplatelet formation were measured at 3 and 5 hours after plating, respectively, as previously described (30, 33).

Megakaryocyte biochemistry

Whole-cell lysates of megakaryocytes stimulated for 10 min with Tpo (50 ng/ml) as well as BSA-nonadherent and fibrinogen-adherent megakaryocytes 3 hours after plating were prepared and analyzed by Western blotting, as previously described (30, 33).

Measurement of serum Tpo concentrations

Serum Tpo concentrations were measured with an ELISA (enzyme-linked immunosorbent assay)–based assay (R&D Systems), as described by the manufacturer.

Tail bleeding assay

Experiments were performed on 17- to 33-g, litter-matched *G6b*$^{+/+}$ and *G6b*$^{-/-}$ mice (aged 8 to 10 weeks), as previously described (59).

Transmission electron microscopy

Platelet-rich plasma was initially fixed with an equal volume of 0.1% glutaraldehyde in 0.1 M sodium cacodylate buffer. Further sample preparation was performed with a similar protocol to that previously described (63). Ultrathin sections (70 to 90 nm) were stained with uranyl acetate and lead citrate and examined with a JEOL 1200EX transmission electron microscope (Centre for Electron Microscopy, University of Birmingham).

Platelet biochemistry

Whole-cell lysates were prepared from washed human and mouse platelets, and proteins were subjected to immunoprecipitation and Western blotting analysis as previously described (64). Washed mouse platelets (5×10^8/ml) were pooled from three to eight *G6b*$^{-/-}$ mice for immunoprecipitation. For deglycosylation experiments, immunoprecipitated samples were incubated with PNGase F (12500 U/ml; New England BioLabs) for 1 hour at 37°C.

Flow cytometry

Washed mouse platelets (1×10^6) were stained for surface glycoproteins with specific antibodies and analyzed with a FACSCalibur flow cytometer and CellQuest software (Becton Dickinson), as previously described (59).

Analysis of platelet aggregation and secretion of ATP

Washed mouse platelets (2×10^8/ml) were analyzed for aggregation and ATP secretion with a lumi-aggregometer (Chrono-Log), as previously described (59). ADP-sensitive, washed mouse platelets were prepared as previously described (65).

Platelet spreading

Platelet spreading on a fibrinogen-coated surface was performed and analyzed as previously described (66).

Platelet adhesion under flow

Anti–coagulated mouse blood [with heparin (5 U/ml) and 40 μM PPACK (Phe-Pro-Arg-chloromethylketone)] was flowed through collagen-coated (100 μg/ml) glass microslide capillaries (1 × 0.1 mm) at a shear rate of 1000 s^{-1} for 4 min at 37°C, as previously described (59). Capillaries were washed for 5 min at 1000 s^{-1} and DIC images were captured. Cells were also stained with 2 μM $DiOC_6$ before flowing, and platelet adhesion and aggregate formation were imaged in real time.

Statistical analysis

The Mann-Whitney *U* test and Student's *t* test were used to compare sample means and determine statistical significance between pairs of samples. A two-way analysis of variance (ANOVA) was used to compare differences between multiple observations of more than one variable. $P < 0.05$ was considered statistically significant in all cases.

Supplementary Material

Refer to Web version on PubMed Central for supplementary material.

Acknowledgments

We thank B. Neel and L. Machesky for invaluable discussions, J. Ware for providing the GPVI-knockout mice, and all members of the Biomedical Services Unit for exceptional technical support. Y.A.S. is a British Heart Foundation (BHF) Intermediate Basic Science Research Fellow. S.P.W. is a BHF Chair.

Funding: Funding for this study was provided by the BHF (A.M., Y.-J.W., J.M., D.B., S.H., S.P.W., and Y.A.S.), Wellcome Trust (B.F. and S.P.W.), and the National Health and Medical Research Council of Australia (E.E.G.).

REFERENCES AND NOTES

1. George JN. Platelets. Lancet. 2000; 355:1531–1539. [PubMed: 10801186]
2. Hartwig JH. The platelet: Form and function. Semin. Hematol. 2006; 43:S94–S100. [PubMed: 16427392]
3. Grozovsky R, Hoffmeister KM, Falet H. Novel clearance mechanisms of platelets. Curr. Opin. Hematol. 2010; 17:585–589. [PubMed: 20729731]
4. Schmitt A, Guichard J, Massè JM, Debili N, Cramer EM. Of mice and men: Comparison of the ultrastructure of megakaryocytes and platelets. Exp. Hematol. 2001; 29:1295–1302. [PubMed: 11698125]
5. Daëron M, Jaeger S, Du Pasquier L, Vivier E. Immunoreceptor tyrosine-based inhibition motifs: A quest in the past and future. Immunol. Rev. 2008; 224:11–43. [PubMed: 18759918]
6. Falati S, Patil S, Gross PL, Stapleton M, Merrill-Skoloff G, Barrett NE, Pixton KL, Weiler H, Cooley B, Newman DK, Newman PJ, Furie BC, Furie B, Gibbins JM. Platelet PECAM-1 inhibits thrombus formation in vivo. Blood. 2006; 107:535–541. [PubMed: 16166583]
7. Wong C, Liu Y, Yip J, Chand R, Wee JL, Oates L, Nieswandt B, Reheman A, Ni H, Beauchemin N, Jackson DE. CEACAM1 negatively regulates platelet-collagen interactions and thrombus growth in vitro and in vivo. Blood. 2009; 113:1818–1828. [PubMed: 19008452]
8. Washington AV, Gibot S, Acevedo I, Gattis J, Quigley L, Feltz R, De La Mota A, Schubert RL, Gomez-Rodriguez J, Cheng J, Dutra A, Pak E, Chertov O, Rivera L, Morales J, Lubkowski J, Hunter R, Schwartzberg PL, McVicar DW. TREM-like transcript-1 protects against inflammation-associated hemorrhage by facilitating platelet aggregation in mice and humans. J. Clin. Invest. 2009; 119:1489–1501. [PubMed: 19436112]
9. Senis YA, Tomlinson MG, García A, Dumon S, Heath VL, Herbert J, Cobbold SP, Spalton JC, Ayman S, Antrobus R, Zitzmann N, Bicknell R, Frampton J, Authi KS, Martin A, Wakelam MJ, Watson SP. A comprehensive proteomics and genomics analysis reveals novel transmembrane proteins in human platelets and mouse megakaryocytes including G6b-B, a novel immunoreceptor tyrosine-based inhibitory motif protein. Mol. Cell. Proteomics. 2007; 6:548–564. [PubMed: 17186946]
10. Steevels TA, Westerlaken GH, Tijssen MR, Coffer PJ, Lenting PJ, Akkerman JW, Meyaard L. Co-expression of the collagen receptors leukocyte-associated immunoglobulin-like receptor-1 and glycoprotein VI on a subset of megakaryoblasts. Haematologica. 2010; 95:2005–2012. [PubMed: 20713462]
11. Xue J, Zhang X, Zhao H, Fu Q, Cao Y, Wang Y, Feng X, Fu A. Leukocyte-associated immunoglobulin-like receptor-1 is expressed on human megakaryocytes and negatively regulates the maturation of primary megakaryocytic progenitors and cell line. Biochem. Biophys. Res. Commun. 2011; 405:128–133. [PubMed: 21216234]
12. Macaulay IC, Tijssen MR, Thijssen-Timmer DC, Gusnanto A, Steward M, Burns P, Langford CF, Ellis PD, Dudbridge F, Zwaginga JJ, Watkins NA, van der Schoot CE, Ouwehand WH. Comparative gene expression profiling of in vitro differentiated megakaryocytes and erythroblasts identifies novel activatory and inhibitory platelet membrane proteins. Blood. 2007; 109:3260–3269. [PubMed: 17192395]

13. Lewandrowski U, Wortelkamp S, Lohrig K, Zahedi RP, Wolters DA, Walter U, Sickmann A. Platelet membrane proteomics: A novel repository for functional research. Blood. 2009; 114:e10–e19. [PubMed: 19436052]
14. de Vet EC, Aguado B, Campbell RD. G6b, a novel immunoglobulin superfamily member encoded in the human major histocompatibility complex, interacts with SHP-1 and SHP-2. J. Biol. Chem. 2001; 276:42070–42076. [PubMed: 11544253]
15. Senis YA, Antrobus R, Severin S, Parguiña AF, Rosa I, Zitzmann N, Watson SP, García A. Proteomic analysis of integrin αIIbβ3 outside-in signaling reveals Src-kinase-independent phosphorylation of Dok-1 and Dok-3 leading to SHIP-1 interactions. J. Thromb. Haemost. 2009; 7:1718–1726. [PubMed: 19682241]
16. Mori J, Pearce AC, Spalton JC, Grygielska B, Eble JA, Tomlinson MG, Senis YA, Watson SP. G6b-B inhibits constitutive and agonist-induced signaling by glycoprotein VI and CLEC-2. J. Biol. Chem. 2008; 283:35419–35427. [PubMed: 18955485]
17. Newland SA, Macaulay IC, Floto AR, de Vet EC, Ouwehand WH, Watkins NA, Lyons PA, Campbell DR. The novel inhibitory receptor G6B is expressed on the surface of platelets and attenuates platelet function in vitro. Blood. 2007; 109:4806–4809. [PubMed: 17311996]
18. Xie T, Rowen L, Aguado B, Ahearn ME, Madan A, Qin S, Campbell RD, Hood L. Analysis of the gene-dense major histocompatibility complex class III region and its comparison to mouse. Genome Res. 2003; 13:2621–2636. [PubMed: 14656967]
19. Italiano JE Jr. Shivdasani RA. Megakaryocytes and beyond: The birth of platelets. J. Thromb. Haemost. 2003; 1:1174–1182. [PubMed: 12871316]
20. Tober J, Koniski A, McGrath KE, Vemishetti R, Emerson R, de Mesy-Bentley KK, Waugh R, Palis J. The megakaryocyte lineage originates from hemangioblast precursors and is an integral component both of primitive and of definitive hematopoiesis. Blood. 2007; 109:1433–1441. [PubMed: 17062726]
21. Ault KA, Knowles C. In vivo biotinylation demonstrates that reticulated platelets are the youngest platelets in circulation. Exp. Hematol. 1995; 23:996–1001. [PubMed: 7635185]
22. Varricchio L, Mancini A, Migliaccio AR. Pathological interactions between hematopoietic stem cells and their niche revealed by mouse models of primary myelofibrosis. Expert Rev. Hematol. 2009; 2:315–334. [PubMed: 20352017]
23. Kaushansky K. The molecular mechanisms that control thrombopoiesis. J. Clin. Invest. 2005; 115:3339–3347. [PubMed: 16322778]
24. Gardiner EE, Karunakaran D, Shen Y, Arthur JF, Andrews RK, Berndt MC. Controlled shedding of platelet glycoprotein (GP)VI and GPIb-IX-V by ADAM family metalloproteinases. J. Thromb. Haemost. 2007; 5:1530–1537. [PubMed: 17445093]
25. Bender M, Hofmann S, Stegner D, Chalaris A, Bösl M, Braun A, Scheller J, Rose-John S, Nieswandt B. Differentially regulated GPVI ectodomain shedding by multiple platelet-expressed proteinases. Blood. 2010; 116:3347–3355. [PubMed: 20644114]
26. Thon JN, Italiano JE. Visualization and manipulation of the platelet and megakaryocyte cytoskeleton. Methods Mol. Biol. 2012; 788:109–125. [PubMed: 22130704]
27. Sabri S, Jandrot-Perrus M, Bertoglio J, Farndale RW, Mas VM, Debili N, Vainchenker W. Differential regulation of actin stress fiber assembly and proplatelet formation by α2β1 integrin and GPVI in human megakaryocytes. Blood. 2004; 104:3117–3125. [PubMed: 15265786]
28. Roskoski R Jr. Src kinase regulation by phosphorylation and dephosphorylation. Biochem. Biophys. Res. Commun. 2005; 331:1–14. [PubMed: 15845350]
29. Cargnello M, Roux PP. Activation and function of the MAPKs and their substrates, the MAPK-activated protein kinases. Microbiol. Mol. Biol. Rev. 2011; 75:50–83. [PubMed: 21372320]
30. Mazharian A, Watson SP, Séverin S. Critical role for ERK1/2 in bone marrow and fetal liver-derived primary megakaryocyte differentiation, motility, and proplatelet formation. Exp. Hematol. 2009; 37:1238–1249. [PubMed: 19619605]
31. Larson MK, Watson SP. Regulation of proplatelet formation and platelet release by integrin $\alpha_{IIb}\beta_3$. Blood. 2006; 108:1509–1514. [PubMed: 16670270]
32. Ghevaert C, Salsmann A, Watkins NA, Schaffner-Reckinger E, Rankin A, Garner SF, Stephens J, Smith GA, Debili N, Vainchenker W, de Groot PG, Huntington JA, Laffan M, Kieffer N,

Ouwehand WH. A nonsynonymous SNP in the ITGB3 gene disrupts the conserved membrane-proximal cytoplasmic salt bridge in the $\alpha_{IIb}\beta_3$ integrin and cosegregates dominantly with abnormal proplatelet formation and macrothrombocytopenia. Blood. 2008; 111:3407–3414. [PubMed: 18065693]

33. Mazharian A, Ghevaert C, Zhang L, Massberg S, Watson SP. Dasatinib enhances megakaryocyte differentiation but inhibits platelet formation. Blood. 2011; 117:5198–5206. [PubMed: 21385851]
34. Italiano JE Jr. Battinelli EM. Selective sorting of alpha-granule proteins. J. Thromb. Haemost. 2009; 7(suppl. 1):173–176. [PubMed: 19630794]
35. Inoue O, Suzuki-Inoue K, Dean WL, Frampton J, Watson SP. Integrin $\alpha_2\beta_1$ mediates outside-in regulation of platelet spreading on collagen through activation of Src kinases and PLCγ2. J. Cell Biol. 2003; 160:769–780. [PubMed: 12615912]
36. Nieswandt B, Watson SP. Platelet-collagen interaction: Is GPVI the central receptor? Blood. 2003; 102:449–461. [PubMed: 12649139]
37. Snell DC, Schulte V, Jarvis GE, Arase K, Sakurai D, Saito T, Watson SP, Nieswandt B. Differential effects of reduced glycoprotein VI levels on activation of murine platelets by glycoprotein VI ligands. Biochem. J. 2002; 368:293–300. [PubMed: 12117414]
38. Fuller GL, Williams JA, Tomlinson MG, Eble JA, Hanna SL, Pöhlmann S, Suzuki-Inoue K, Ozaki Y, Watson SP, Pearce AC. The C-type lectin receptors CLEC-2 and Dectin-1, but not DC-SIGN, signal via a novel YXXL-dependent signaling cascade. J. Biol. Chem. 2007; 282:12397–12409. [PubMed: 17339324]
39. Watson SP, Auger JM, McCarty OJ, Pearce AC. GPVI and integrin αIIbβ3 signaling in platelets. J. Thromb. Haemost. 2005; 3:1752–1762. [PubMed: 16102042]
40. Nieswandt B, Bergmeier W, Schulte V, Rackebrandt K, Gessner JE, Zirngibl H. Expression and function of the mouse collagen receptor glycoprotein VI is strictly dependent on its association with the FcRγ chain. J. Biol. Chem. 2000; 275:23998–24002. [PubMed: 10825177]
41. May F, Hagedorn I, Pleines I, Bender M, Vögtle T, Eble J, Elvers M, Nieswandt B. CLEC-2 is an essential platelet-activating receptor in hemostasis and thrombosis. Blood. 2009; 114:3464–3472. [PubMed: 19641185]
42. Kato K, Kanaji T, Russell S, Kunicki TJ, Furihata K, Kanaji S, Marchese P, Reininger A, Ruggeri ZM, Ware J. The contribution of glycoprotein VI to stable platelet adhesion and thrombus formation illustrated by targeted gene deletion. Blood. 2003; 102:1701–1707. [PubMed: 12738669]
43. Dhanjal TS, Pendaries C, Ross EA, Larson MK, Protty MB, Buckley CD, Watson SP. A novel role for PECAM-1 in megakaryocytokinesis and recovery of platelet counts in thrombocytopenic mice. Blood. 2007; 109:4237–4244. [PubMed: 17234740]
44. Dhanjal TS, Ross EA, Auger JM, McCarty OJ, Hughes CE, Senis YA, Buckley CD, Watson SP. Minimal regulation of platelet activity by PECAM-1. Platelets. 2007; 18:56–67. [PubMed: 17365855]
45. Tang X, Tian L, Esteso G, Choi SC, Barrow AD, Colonna M, Borrego F, Coligan JE. Leukocyte-associated Ig-like receptor-1-deficient mice have an altered immune cell phenotype. J. Immunol. 2012; 188:548–558. [PubMed: 22156345]
46. Strom TS. The thrombocytopenia of WAS: A familial form of ITP? Immunol. Res. 2009; 44:42–53. [PubMed: 18854955]
47. Falet H, Marchetti MP, Hoffmeister KM, Massaad MJ, Geha RS, Hartwig JH. Platelet-associated IgAs and impaired GPVI responses in platelets lacking WIP. Blood. 2009; 114:4729–4737. [PubMed: 19692704]
48. Mazharian A, Thomas SG, Dhanjal TS, Buckley CD, Watson SP. Critical role of Src-Syk-PLCγ2 signaling in megakaryocyte migration and thrombopoiesis. Blood. 2010; 116:793–800. [PubMed: 20457868]
49. Schwer HD, Lecine P, Tiwari S, Italiano JE Jr. Hartwig JH, Shivdasani RA. A lineage-restricted and divergent β-tubulin isoform is essential for the biogenesis, structure and function of blood platelets. Curr. Biol. 2001; 11:579–586. [PubMed: 11369202]
50. Avecilla ST, Hattori K, Heissig B, Tejada R, Liao F, Shido K, Jin DK, Dias S, Zhang F, Hartman TE, Hackett NR, Crystal RG, Witte L, Hicklin DJ, Bohlen P, Eaton D, Lyden D, de Sauvage F,

Rafii S. Chemokine-mediated interaction of hematopoietic progenitors with the bone marrow vascular niche is required for thrombopoiesis. Nat. Med. 2004; 10:64–71. [PubMed: 14702636]

51. Thon JN, Montalvo A, Patel-Hett S, Devine MT, Richardson JL, Ehrlicher A, Larson MK, Hoffmeister K, Hartwig JH, Italiano JE Jr. Cytoskeletal mechanics of proplatelet maturation and platelet release. J. Cell Biol. 2010; 191:861–874. [PubMed: 21079248]
52. Bergmeier W, Piffath CL, Cheng G, Dole VS, Zhang Y, von Andrian UH, Wagner DD. Tumor necrosis factor-α–converting enzyme (ADAM17) mediates GPIbα shedding from platelets in vitro and in vivo. Circ. Res. 2004; 95:677–683. [PubMed: 15345652]
53. Barford D, Neel BG. Revealing mechanisms for SH2 domain mediated regulation of the protein tyrosine phosphatase SHP-2. Structure. 1998; 6:249–254. [PubMed: 9551546]
54. Eck MJ, Pluskey S, Trüb T, Harrison SC, Shoelson SE. Spatial constraints on the recognition of phosphoproteins by the tandem SH2 domains of the phosphatase SH-PTP2. Nature. 1996; 379:277–280. [PubMed: 8538796]
55. Hof P, Pluskey S, Dhe-Paganon S, Eck MJ, Shoelson SE. Crystal structure of the tyrosine phosphatase SHP-2. Cell. 1998; 92:441–450. [PubMed: 9491886]
56. Pluskey S, Wandless TJ, Walsh CT, Shoelson SE. Potent stimulation of SH-PTP2 phosphatase activity by simultaneous occupancy of both SH2 domains. J. Biol. Chem. 1995; 270:2897–2900. [PubMed: 7531695]
57. Yang J, Cheng Z, Niu T, Liang X, Zhao ZJ, Zhou GW. Structural basis for substrate specificity of protein-tyrosine phosphatase SHP-1. J. Biol. Chem. 2000; 275:4066–4071. [PubMed: 10660565]
58. Yang J, Liu L, He D, Song X, Liang X, Zhao ZJ, Zhou GW. Crystal structure of human protein-tyrosine phosphatase SHP-1. J. Biol. Chem. 2003; 278:6516–6520. [PubMed: 12482860]
59. Senis YA, Tomlinson MG, Ellison S, Mazharian A, Lim J, Zhao Y, Kornerup KN, Auger JM, Thomas SG, Dhanjal T, Kalia N, Zhu JW, Weiss A, Watson SP. The tyrosine phosphatase CD148 is an essential positive regulator of platelet activation and thrombosis. Blood. 2009; 113:4942–4954. [PubMed: 19246339]
60. Lecine P, Blank V, Shivdasani R. Characterization of the hematopoietic transcription factor NF-E2 in primary murine megakaryocytes. J. Biol. Chem. 1998; 273:7572–7578. [PubMed: 9516460]
61. Dumon S, Heath VL, Tomlinson MG, Göttgens B, Frampton J. Differentiation of murine committed megakaryocytic progenitors isolated by a novel strategy reveals the complexity of GATA and Ets factor involvement in megakaryocytopoiesis and an unexpected potential role for GATA-6. Exp. Hematol. 2006; 34:654–663. [PubMed: 16647571]
62. McCormack MP, Hall MA, Schoenwaelder SM, Zhao Q, Ellis S, Prentice JA, Clarke AJ, Slater NJ, Salmon JM, Jackson SP, Jane SM, Curtis DJ. A critical role for the transcription factor Scl in platelet production during stress thrombopoiesis. Blood. 2006; 108:2248–2256. [PubMed: 16763211]
63. Konopatskaya O, Gilio K, Harper MT, Zhao Y, Cosemans JM, Karim ZA, Whiteheart SW, Molkentin JD, Verkade P, Watson SP, Heemskerk JW, Poole AW. PKCα regulates platelet granule secretion and thrombus formation in mice. J. Clin. Invest. 2009; 119:399–407. [PubMed: 19147982]
64. Pearce AC, Senis YA, Billadeau DD, Turner M, Watson SP, Vigorito E. Vav1 and Vav3 have critical but redundant roles in mediating platelet activation by collagen. J. Biol. Chem. 2004; 279:53955–53962. [PubMed: 15456756]
65. Ohlmann P, Eckly A, Freund M, Cazenave JP, Offermanns S, Gachet C. ADP induces partial platelet aggregation without shape change and potentiates collagen-induced aggregation in the absence of Gαq. Blood. 2000; 96:2134–2139. [PubMed: 10979958]
66. McCarty OJ, Larson MK, Auger JM, Kalia N, Atkinson BT, Pearce AC, Ruf S, Henderson RB, Tybulewicz VL, Machesky LM, Watson SP. Rac1 is essential for platelet lamellipodia formation and aggregate stability under flow. J. Biol. Chem. 2005; 280:39474–39484. [PubMed: 16195235]

Europe PMC Funders Author Manuscripts

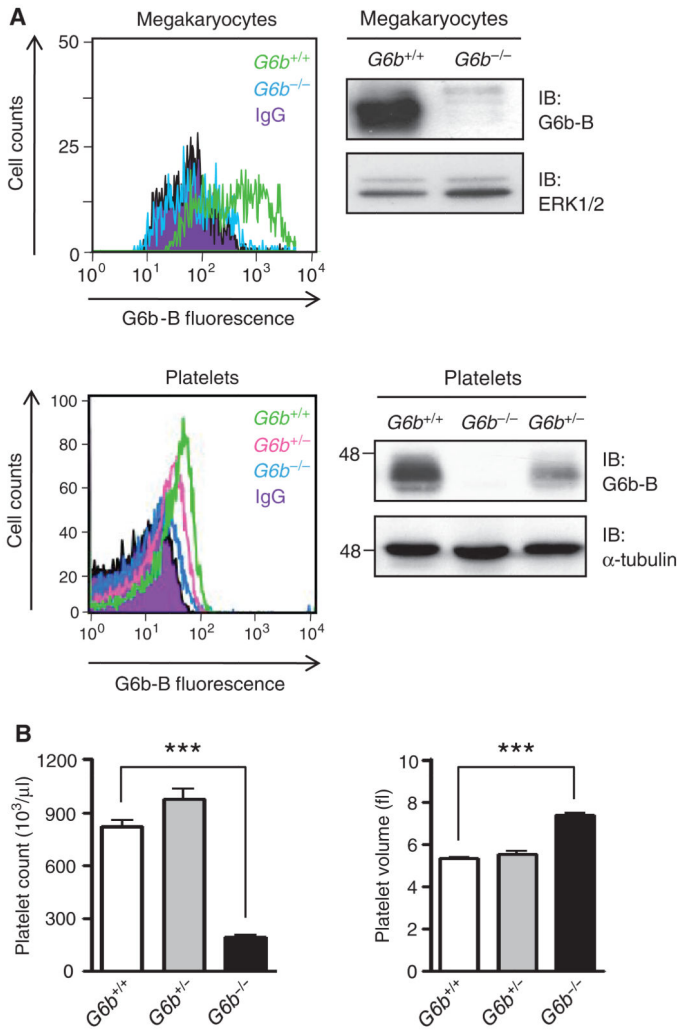

Fig. 1. G6b-B–deficient mice are markedly macrothrombocytopenic.

(**A**) Flow cytometric and Western blotting analysis of G6b-B in mature bone marrow–derived mouse megakaryocytes (top) and platelets (bottom) from wild-type ($G6b^{+/+}$), $G6b^{+/-}$, and $G6b^{-/-}$ mice. Representative histograms for four mice of each genotype are shown. Representative blots from three experiments are shown. (**B**) Platelet counts (left) and platelet volumes (right) were determined in mice of the following genotypes: $G6b^{+/+}$ ($n = 24$ mice), $G6b^{+/-}$ ($n = 10$ mice), and $G6b^{-/-}$ ($n = 22$ mice). Data are means ± SEM. ***$P <$ 0.001.

Europe PMC Funders Author Manuscripts

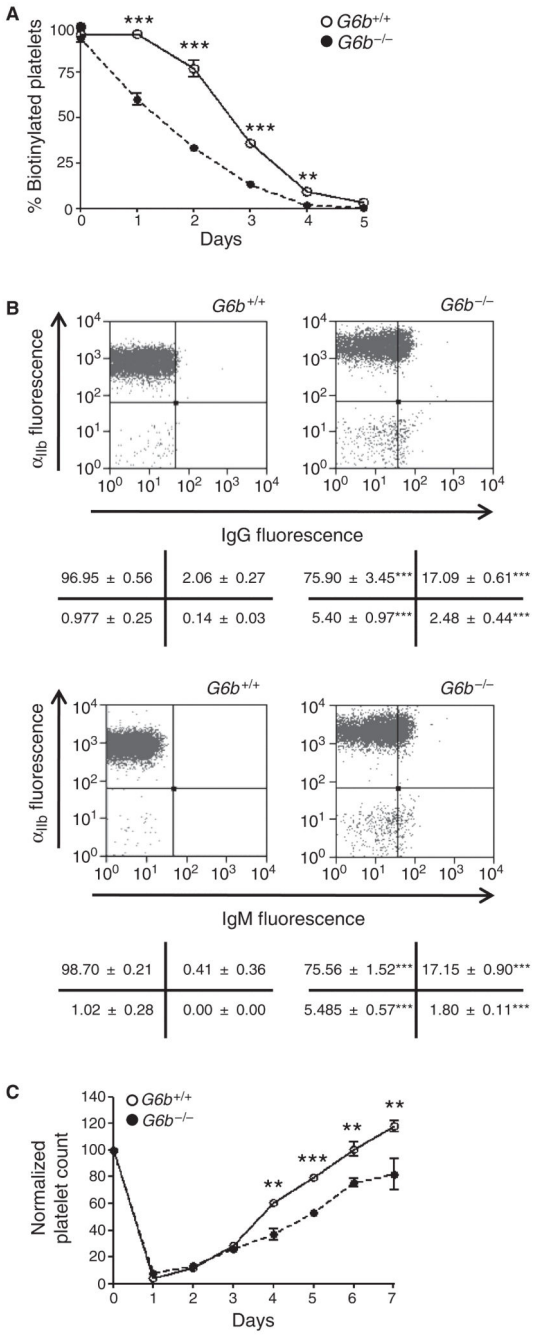

Fig. 2. Increased platelet turnover in G6b-B–deficient mice.

(**A**) Platelet half-life is reduced in *G6b*$^{-/-}$ mice. The percentage of biotinylated platelets in whole blood from age-matched wild-type (*G6b*$^{+/+}$) and *G6b*$^{-/-}$ mice was quantified daily by flow cytometry, after injection of biotin-*N*-hydroxysuccinimide (n = 3 to 5 mice per time point). Data are means ± SEM. $^{**}P < 0.01$; $^{***}P < 0.001$. (**B**) G6b-B–deficient platelets have increased surface IgG and IgM abundance. Platelets from wild-type (*G6b*$^{+/+}$) and *G6b*$^{-/-}$ mice were double-stained for α_{IIb} and either IgG (top) or IgM (bottom) and analyzed by flow cytometry. Representative histograms for four mice of each genotype are shown.

The percentages of positive cells in each quadrant are shown below each histogram. Data are means ± SEM. ***$P < 0.001$. (**C**) Delay in platelet recovery after anti-GPIbα antibody–induced thrombocytopenia in *G6b*$^{-/-}$ mice ($n = 3$ to 5 mice per time point). Data are means ± SEM. **$P < 0.01$; ***$P < 0.001$.

Europe PMC Funders Author Manuscripts

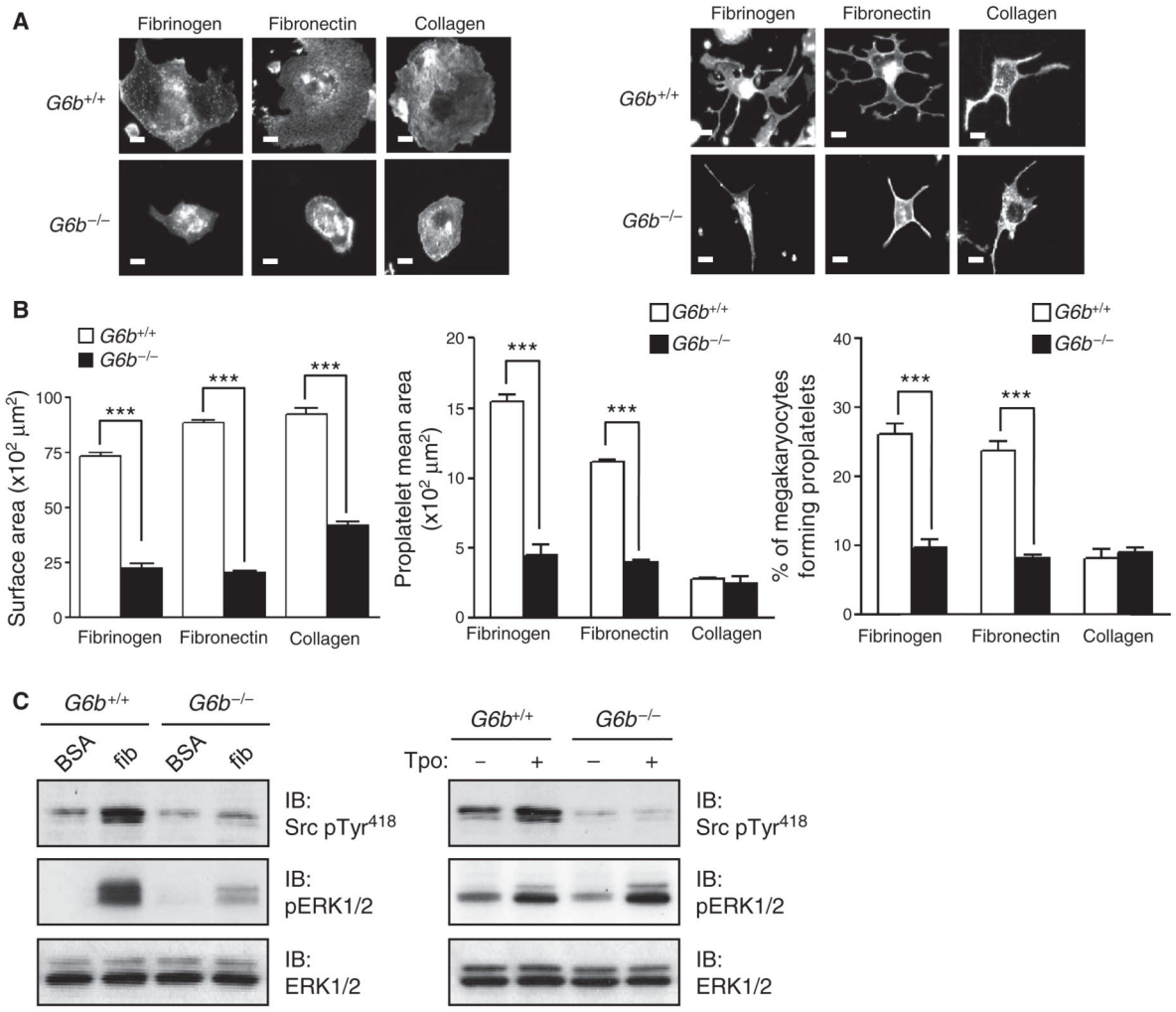

Fig. 3. Reduced proplatelet formation by G6b-B–deficient megakaryocytes.

(**A**) Reduced spreading (left) and proplatelet formation (right) of G6b-B–deficient megakaryocytes. Representative images from four to six mice of each genotype are shown. Scale bar, 20 µm. (**B**) Surface area, mean proplatelet area, and percentage of megakaryocytes forming proplatelets were quantified for four to six mice of each genotype. Data are means ± SD. ***$P < 0.001$. (**C**) Reduced signaling in G6b-B–deficient megakaryocytes. (Left) Whole-cell lysates of bovine serum albumin (BSA)–nonadherent and fibrinogen-adherent (fib) wild-type ($G6b^{+/+}$) and $G6b^{-/-}$ megakaryocytes were analyzed by Western blotting with antibodies against Src pTyr^{418}, pERK1/2, and total ERK1/2. Representative blots from three experiments are shown. (Right) Whole-cell lysates of resting (−) and Tpo-stimulated (+; 50 ng/ml for 10 min) wild-type ($G6b^{+/+}$) and $G6b^{-/-}$ megakaryocytes were analyzed by Western blotting with antibodies against Src pTyr^{418} pERK1/2 and total ERK1/2. Representative blots from three experiments are shown.

Europe PMC Funders Author Manuscripts

Europe PMC Funders Author Manuscripts

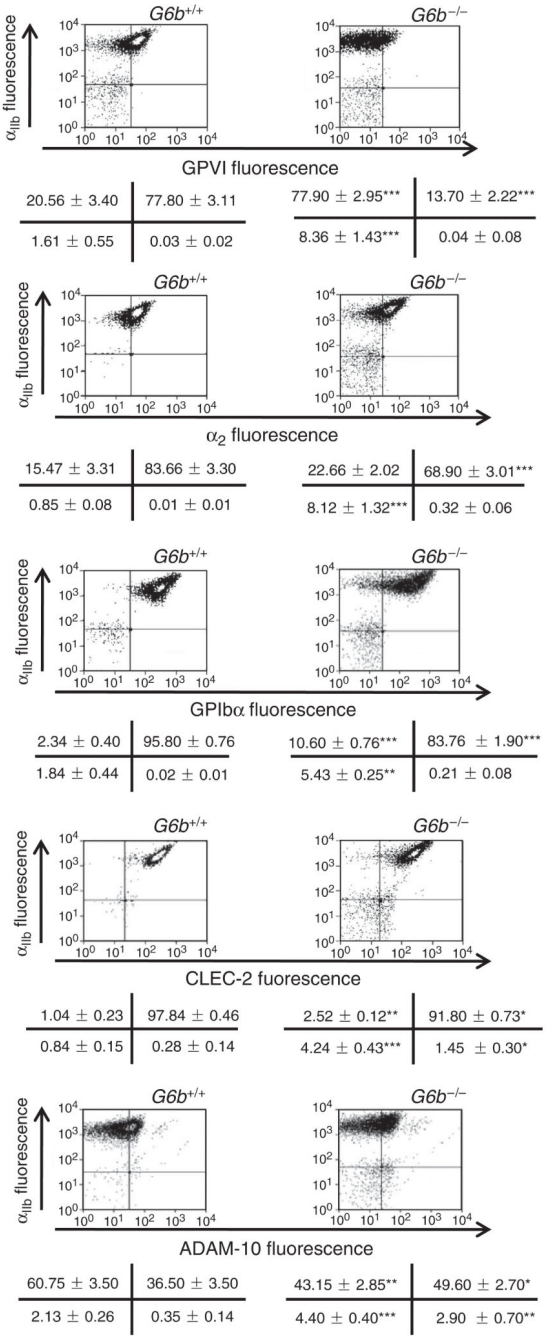

Fig. 4. Altered surface glycoprotein abundance in G6b-B–deficient platelets.

Platelets were double-stained for α_{IIb} integrin and GPVI, α_2 integrin, GPIbα, CLEC-2, or ADAM-10 and were analyzed by flow cytometry. Representative histograms from six mice for each genotype are shown. The percentages of positive cells in each quadrant are shown below the histograms. Data are means ± SEM. $*P < 0.05$; $**P < 0.01$; $***P < 0.001$.

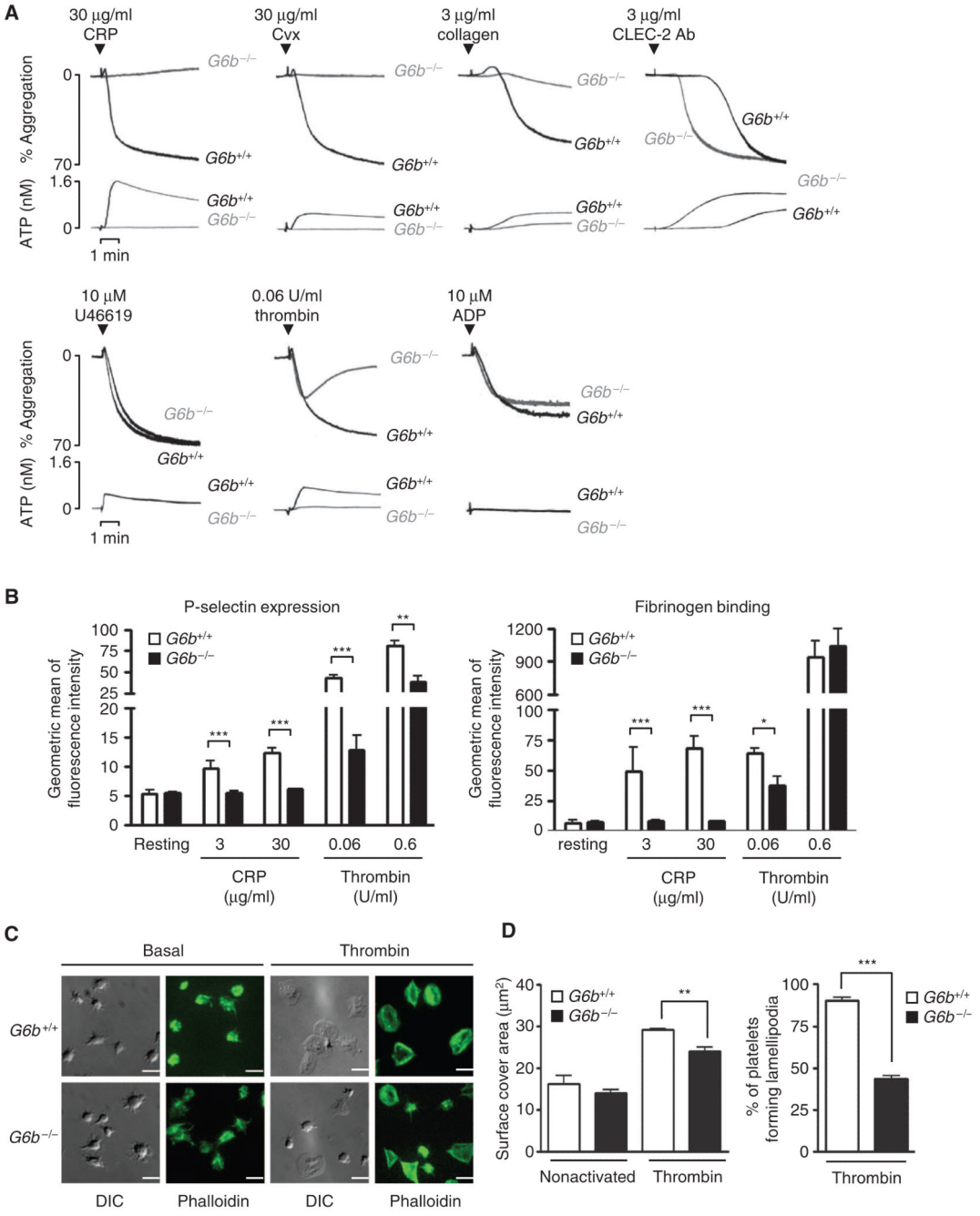

Fig. 5. Aberrant platelet functions in G6b-B–deficient mice.

(**A**) Aggregation and ATP secretion of washed platelets (2×10^8/ml) from wild-type (*G6b*$^{+/+}$) and *G6b*$^{-/-}$ mice were measured by lumi-aggregometry. Agonists and concentrations are indicated. CRP, collagen-related peptide; Cvx, convulxin. Representative traces from four to six mice of each genotype are shown. (**B**) Impaired surface expression of P-selectin and fibrinogen binding. Surface P-selectin abundance and fibrinogen binding in response to low and high concentrations of CRP and thrombin were measured by flow cytometry ($n = 5$ mice). Data are means ± SD. *$P < 0.05$; **$P < 0.01$; ***$P < 0.001$. (**C**)

Basal and thrombin (0.1 U/ml)–activated platelets from wild-type ($G6b^{+/+}$) and $G6b^{-/-}$ mice were plated on a fibrinogen-coated surface. Representative differential interference contrast (DIC) and phalloidin-stained images from four mice are shown. Scale bar, 5 μm. (**D**) The surface area of individual adherent platelets and the percent of platelets forming lamellipodia were quantified. Data are means ± SD. $^{**}P < 0.01$; $^{***}P < 0.001$.

Europe PMC Funders Author Manuscripts

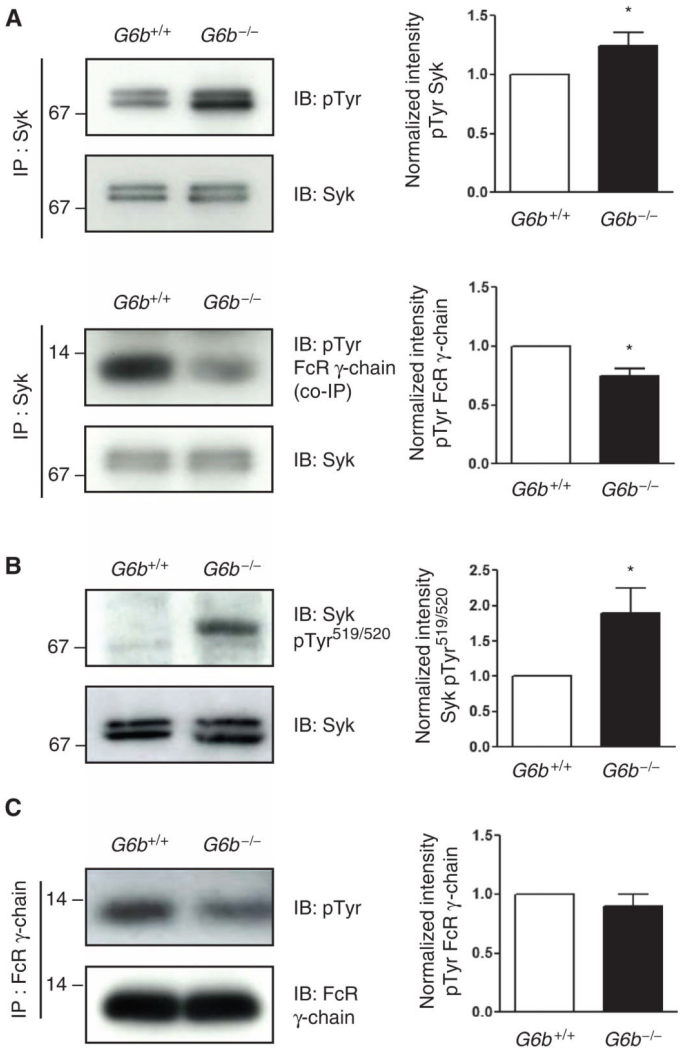

Fig. 6. Aberrant tyrosine phosphorylation in G6b-B–deficient platelets.

(**A**) The extent of phosphorylation of Syk is enhanced in resting G6b-B–deficient platelets. Representative Western blot (IB) of Syk immunoprepitated (IP) from resting wild-type (*G6b*$^{+/+}$) and *G6b*$^{-/-}$ platelets and analyzed with an anti-pTyr antibody. Membranes were then stripped and incubated with an anti-Syk antibody. Quantification of band intensities of pTyr-Syk and coimmunoprecipitated (co-IP) pTyr-FcR γ-chain is shown in the bar charts. Data are the means ± SD from four experiments, normalized to the loading control. *$P <$ 0.05. (**B**) Representative Western blot of whole-cell lysates from resting wild-type (*G6b*$^{+/+}$) and *G6b*$^{-/-}$ platelets analyzed with an anti-Syk pTyr$^{519/520}$ antibody. Membranes were stripped and then incubated with an anti-Syk antibody. Quantification of band intensities of Syk pTyr$^{519/520}$ from four experiments, normalized to the loading control; data are presented in the bar graph as means ± SD. *$P < 0.05$. (**C**) Representative Western blot of the FcR γ-chain immunoprecipitated from resting wild-type (*G6b*$^{+/+}$) and *G6b*$^{-/-}$ platelets and analyzed with an anti-pTyr antibody. Membranes were then stripped and incubated with an anti–FcR γ-chain antibody. Quantification of band intensities of FcR γ-chain is shown in the

bar graph chart. Data are mean ± SD from four experiments, normalized to the loading control.

Europe PMC Funders Author Manuscripts

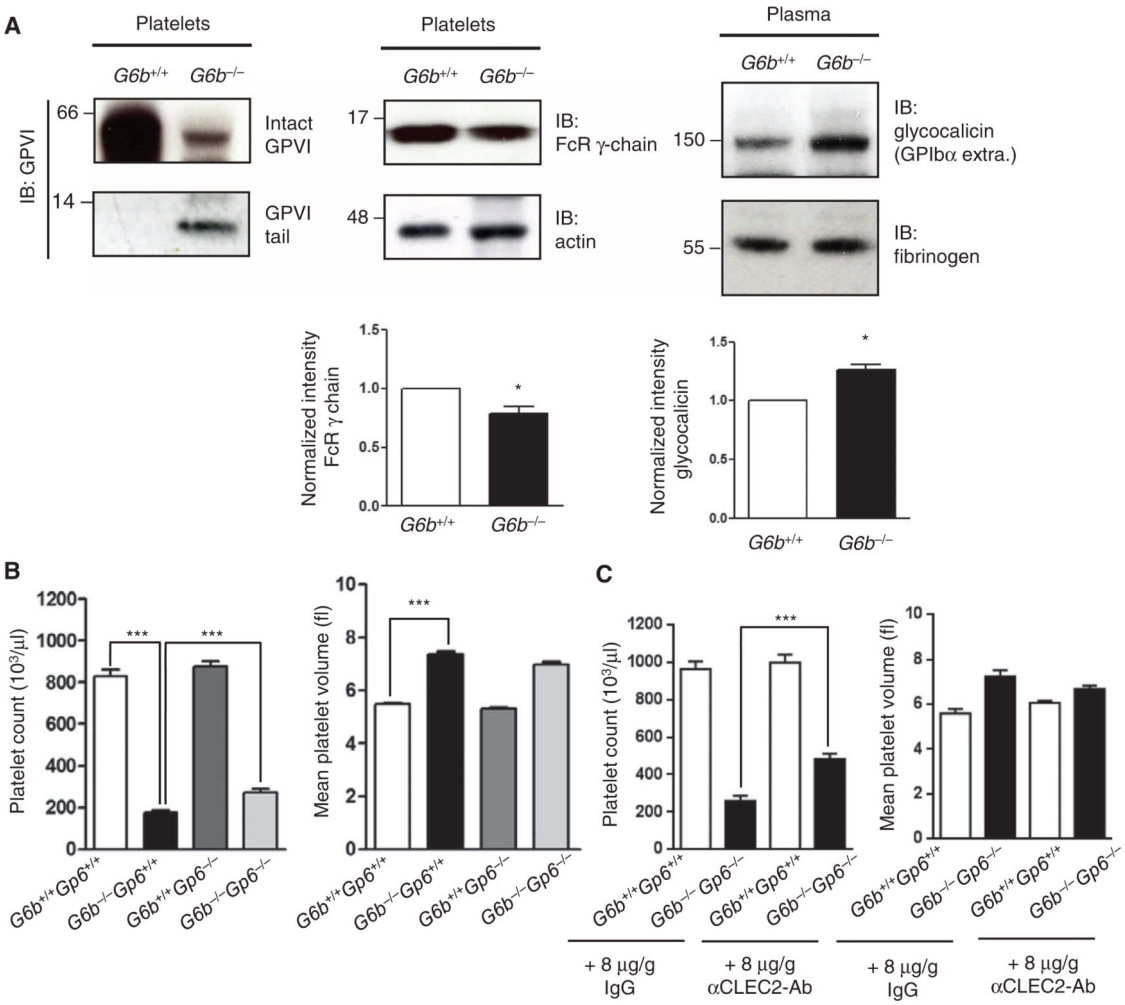

Fig. 7. Ablation of GPVI and CLEC-2 partially rescues macrothrombocytopenia in G6b-B–deficient mice.

(**A**) Enhanced GPVI and GPIbα shedding in G6b-B–deficient mice.(Left) Platelet lysates from wild-type (*G6b*$^{+/+}$) and *G6b*$^{-/-}$ mice were analyzed by Western blotting (IB) with anti–GPVI cytoplasmic tail (GPVI tail antibody). Full-length GPVI (intact GPVI) and the sheddase-generated C-terminal tail (GPVI tail) are indicated. Representative blots are from four to six mice of each genotype. (Middle) Platelet lysates were analyzed by Western blotting with antibodies against the FcR γ-chain and actin. Representative blots are from four to six mice of each genotype, and quantification of FcR γ-chain is shown in the bargraph. Data are means ± SD. **P* < 0.05. (Right) Representative Western blots showing glycocalicin in plasma from wild-type (*G6b*$^{+/+}$) and *G6b*$^{-/-}$ mice. Blots were then stripped and analyzed for fibrinogen. Quantification of glycocalicin [GPIbα extracellular region (GPIbα extra.)] from eight mice for each genotype is shown in the bar graph. Data are means ± SD. **P* < 0.05. (**B**) Partial rescue of platelet counts in *G6b*/*Gp6* DKO mice. Platelet counts (left) and platelet volumes (right) were measured in *G6b*/*Gp6* DKO (*G6b*$^{-/-}$Gp6$^{-/-}$), GPVI-knockout (*G6b*$^{+/+}$Gp6$^{-/-}$), and litter-matched control mice (*G6b*$^{+/+}$Gp6$^{+/+}$). Data are from 17 to 32 mice of each genotype and are presented as means ± SEM. ****P* < 0.001. (**C**)

Europe PMC Funders Author Manuscripts

Depletion of CLEC-2 partially rescues reduced platelet counts in *G6b*$^{-/-}$Gp6$^{-/-}$ mice. Platelet counts (left) and platelet volumes (right) were measured in mice treated with anti–CLEC-2 antibody or rat IgG1 isotype control. Data are means ± SEM from seven mice of each genotype. ***$P < 0.001$.

Europe PMC Funders Author Manuscripts

Europe PMC Funders Author Manuscripts

Table 1

Surface glycoprotein expression in bone marrow–derived megakaryocytes.

Surface glycoproteins	Immature megakaryocytes		Mature megakaryocytes	
	G6b$^{+/+}$ (mean ± SEM) (*n* = 4)	*G6b*$^{-/-}$ (mean ± SEM) (*n* = 4)	*G6b*$^{+/+}$ (mean ± SEM) (*n* = 4–8)	*G6b*$^{-/-}$ (mean ± SEM) (*n* = 4–8)
G6b-B	2.24 ± 0	1.10 ± 0	24 ± 5	2 ± 0**
CD34	111 ± 24	153 ± 2.2	63 ± 9	77 ± 8
$\alpha_{IIb}\beta_3$ integrin	93.50 ± 15.60	94.15 ± 10.30	270 ± 29	275 ± 34
GPVI	4.90 ± 0.9	5.12 ± 1.52	66 ± 15	25 ± 10**
α_2 integrin	2.50 ± 1	3.55 ± 2.53	32 ± 2	13 ± 2**
GPIbα	4.57 ± 0.39	5.50 ± 1.20	88 ± 9	22 ± 10**
ADAM-10	8.62 ± 0.40	7.68 ± 0.43	29 ± 5	50 ± 6**
CLEC-2	4.15 ± 1.50	5.35 ± 1.10	31 ± 2	32 ± 3

** $P < 0.01$.

Europe PMC Funders Author Manuscripts

Table 2

Surface glycoprotein expression in washed platelets.

Surface glycoproteins	*G6b*$^{+/+}$ (mean ± SEM) (*n* = 6–13)	*G6b*$^{-/-}$ (mean ± SEM) (*n* = 7–14)
GPVI	42.00 ± 2.80	6.39 ± 0.87***
α_2 integrin	3.03 ± 0.23	2.28 ± 0.22*
$\alpha_{IIb}\beta_3$ integrin	359.14 ± 11.44	354.74 ± 21.80
GPIbα	72.53 ± 3.67	60.02 ± 3.64
ADAM-10	15.09 ± 1.76	14.23 ± 1.30
CLEC-2	18.48 ± 0.66	20.09 ± 0.78

*$P < 0.05$; ***$P < 0.001$.